phys. stat. sol. (b) **223**, 75 (2001)

Subject classification: 71.20.Nr; 78.20.Ci; S7.15

Band Anticrossing in III–N–V Alloys

W. SHAN*) (a), W. WALUKIEWICZ (a), K. M. YU (a), J. W. AGER III (a), E. E. HALLER (a), J. F. GEISZ (b), D. J. FRIEDMAN (b), J. M. OLSON (b), S. R. KURTZ (b), H. P. XIN (c), and C. W. TU (c)

(a) Materials Sciences Division, Lawrence Berkeley National Laboratory, Berkeley, CA 94720, USA

(b) National Renewable Energy Laboratory, Golden, CO 80401, USA

(c) Department of Electrical and Computer Engineering, University of California at San Diego, La Jolla, CA 92093, USA

(Received October 2, 2000)

Recent high hydrostatic pressure experiments have shown that incorporation of small amounts of nitrogen into conventional III–V compounds to form III–N–V alloys leads to splitting of the conduction band into two subbands. The downward shift of the lower subband edge is responsible for the observed, large reduction of the fundamental band gaps in III–N–V alloys. The observed effects were explained by an anticrossing interaction between the conduction band states close to the center of the Brillouin zone and localized nitrogen states. The interaction leads to a change in the nature of the fundamental from the indirect gap in GaP to a direct gap in GaNP. The predictions of the band anticrossing model of enlarged electron effective mass and enhanced donor activation efficiency were confirmed by experiments in GaInNAs alloys.

Introduction Doping of conventional group III–V semiconductors with low, impurity-like concentrations of nitrogen introduces highly localized acceptor levels [1]. In GaAs the dispersionless nitrogen level is resonant with the conduction band and is located at about 1.6 to 1.7 eV above the valence band edge. In GaP the level is located slightly below the lowest conduction band edges at X points of the Brillouin zone [1–3]. The electronic band structure of the host crystal is not affected by these low, impurity-like nitrogen concentrations. However, it has been shown that incorporation of higher, alloy-like N concentrations to form III–N–V alloys results in a profound reduction of the fundamental band-gap energy. A reduction of the band gap of more than 100 meV per atomic percentage nitrogen was observed in GaNAs [4]. Similar gap reductions were also observed in other III–N–V semiconductor alloys [5–15]. The strong dependence of the band gap on the N content offers a possibility to use the N-containing alloys for a variety of long wavelength optoelectronic devices [9] and in hybrid solar cell designs [14, 15].

It is commonly accepted that the unexpectedly strong effect of N on the band gap is related to the fact that replacement of atoms such as As or P with much smaller and more electronegative N atoms leads to a large, local perturbation of the crystal lattice potential. However, despite years of extensive experimental and theoretical studies

*) Present address: OptiWork, Inc. Fremont, California 94538, USA.

[4–23], there has been no general consensus on the proper description of the observed effects of N incorporation on the electronic structure of III–N–V alloys. Many of the early experiments on III–N–V alloys were analyzed in terms of the phenomenological Quantum Dielectric Theory [16, 17]. Later, several groups have performed microscopic band structure calculations [18–21]. The calculations could not be easily compared with experiments as they have encountered a problem with a proper treatment of the random atom distributions in the alloys. Recently the band gap bowing coefficients were calculated using Local Density Approximation. The authors argued that in GaNAs alloys the large bowing coefficient is determined by a charge exchange resulting from a replacement of As with N atoms and by structural relaxation of the alloys [20].

All these theoretical calculations were dealing exclusively with the most extensively studied and easily experimentally observed effect of the N-induced band gap reduction in III–N–V alloys. The situation has changed recently because it has been discovered that, in addition to the band gap reduction, incorporation of N leads to the appearance of a new high-energy absorption edge in GaInNAs alloys [24, 25]. These experimental observations have been explained by the band anticrossing (BAC) model that considers the interaction between localized N states and the extended states of the host semiconductor matrix. In this paper we will review our recent experimental and theoretical results obtained on a number of semiconductor alloys. We show that the BAC model is generally applicable to all alloy systems exhibiting very large band gap bowing coefficients. We also present experimental confirmation of the effects predicted by the BAC model.

Experimental The III–N–V alloy samples used in this work include GaNAs, GaInNAs, and GaNP. The GaNAs and GaInNAs samples are epitaxial layers grown at 2.4–7 μm/h between 550 and 650 °C on GaAs substrates by metalorganic vapor phase epitaxy (MOCVD) using dimethylhydrazine as nitrogen source. The GaNP samples were grown at 550 °C on GaP substrates by gas-source molecular beam epitaxy (MBE) using a rf plasma nitrogen radical beam source. The layer thickness varies from 0.5 to 5.0 μm. The nitrogen content of these samples was determined using secondary ion mass spectroscopy (SIMS) and indirectly via the change of the lattice constant measured by reflection (004) double-crystal X-ray diffraction.

Optical measurements including conventional absorption, photoluminescence (PL), and photo-modulation spectroscopy were performed at room temperature. The optical absorption measurements were carried out using a Cary 2390 spectrophotometer. The experimental setup for the PL measurements consisted of an Ar^+ laser (5145 Å line) as an excitation source and a 1.0 m double-grating monochromator with a lock-in amplification and data acquisition system. For the modulation spectroscopy, quasi-monochromatic light from a halogen tungsten lamp dispersed by a 0.5 m monochromator was focused on the samples as a probe beam. A chopped HeCd laser beam (either 3250 or 4420 Å) provided the modulation. Signals were detected by a Si photodiode using a phase-sensitive lock-in amplification system. Application of hydrostatic pressure was accomplished by mounting small sample chips with sizes of $\approx 200 \times 200$ μm^2 into gasketed diamond anvil cells.

Band Anticrossing Model It is well known that an isolated N atom introduces a localized state with energy level E_N in conventional III–V materials. In most cases, this

level is located very close to the conduction band edge. It lies at about 0.25 eV above the conduction band edge in GaAs and less than 0.1 eV below the conduction band edge in GaP. A weak pressure dependence of the N energy level was observed in GaAs compared to the conduction-band edge. The level was also found to move into the band gap when GaAs is alloyed with AlAs [26]. The highly localized nature of the N states suggests weak hybridization between the orbits of N atoms and the extended states, $E_{\mathrm{M}}(k)$, of the semiconductor matrix.

In considering the problem of group III–N–V alloys, we assume that N atoms substituted on the group V elements are randomly distributed in a crystal lattice and are only weakly coupled to the extended states of the host semiconductor matrix [24, 27]. The eigenvalue problem can then be written as

$$\begin{vmatrix} E - E_{\mathrm{M}}(k) & -V_{\mathrm{NM}} \\ -V_{\mathrm{NM}} & E - E_{\mathrm{N}} \end{vmatrix} = 0\,, \tag{1}$$

where $V_{\mathrm{NM}} = \langle k|\, V\, |\mathrm{N}\rangle$ is the matrix element describing the coupling between N-states and the extended conduction-band states, $V = \Sigma_s\, U(\mathbf{r} - \mathbf{R}_s)$, and $U(\mathbf{r} - \mathbf{R}_s)$ is the potential introduced by an N atom on an $\mathbf{R}_s$ site. The solution of Eq. (1) takes the form

$$E_{\pm}(k) = \{(E_{\mathrm{N}} + E_{\mathrm{M}}(k)) \pm [(E_{\mathrm{N}} - E_{\mathrm{M}}(k))^2 + 4(V_{\mathrm{NM}})^2]^{1/2}\}/2\,, \tag{2}$$

where the squared matrix element coupling k and N states is given by

$$\begin{aligned} |V_{\mathrm{NM}}|^2 &= \langle k|\, V\, |N\rangle\, \langle N|\, V\, |k\rangle \\ &= \Sigma_s \Sigma_{s'} \iint V^{-2} \mathrm{d}\mathbf{r}\, \mathrm{d}\mathbf{r}'\, e^{i\mathbf{k}\mathbf{r}}\, U^*(\mathbf{r} - \mathbf{R}_s)\, \Psi_N^*(\mathbf{r} - \mathbf{R}_s)\, U(\mathbf{r}' - \mathbf{R}_{s'})\, \Psi_N(\mathbf{r}' - \mathbf{R}_{s'})\, \mathrm{e}^{-i\mathbf{k}\mathbf{r}'}\,. \end{aligned} \tag{3}$$

$\Psi_{\mathrm{N}}(\mathbf{r})$ is the wavefunction of an N state localized on the substitutional site. Equation (3) is valid only for low N concentrations when there is no appreciable overlap between functions $S(\mathbf{r} - \mathbf{R}_s) = U(\mathbf{r} - \mathbf{R}_s)\ \Psi_{\mathrm{N}}(\mathbf{r} - \mathbf{R}_s)$ located on different sites. Assuming an exponential form $S(\mathbf{r} - \mathbf{R}_s) \sim \exp\,[-\,|\mathbf{r} - \mathbf{R}_s|\ k_L]$, where k_L is the measure of the spatial extent of function S, ne finds from Eq. (3)

$$|V_{\mathrm{NM}}|^2 = |S(k)|^2\, \{\Sigma_s \Sigma_{s'} \exp\,[\mathbf{i}\mathbf{k}\,(\mathbf{R}_s - \mathbf{R}_{s'})]\}\,, \tag{4}$$

where the Fourier transform of $S(\mathbf{r})$ is given by $S(k) = (k_L)^2/[(k_L)^2 + k^2]$.

The double sum in Eq. (4) has to be averaged over all possible N atom configurations in the host crystal lattice. For a random distribution it equals the total number of substitutional N atoms which is proportional to the molar fraction of N in the alloys. Therefore the matrix element describing the hybridization between N states and the conduction-band states of the semiconductor matrix is given by

$$V_{\mathrm{NM}} = C_{\mathrm{NM}} x^{1/2}\,, \tag{5}$$

where C_{NM} is a constant dependent on the semiconductor matrix and x is the mole fraction of substitutional N.

The interaction of the conduction-band edge with the dispersionless N level results in a characteristic level anticrossing that leads to a splitting of the conduction band into two highly nonparabolic subbands, $E_-\ (k)$ and $E_+(k)$. Figure 1 shows an example of the calculated structure of the two conduction subbands. The band anticrossing (BAC) model predicts a new interband transition associated with the E_+ minimum, in addition to the interband transitions from the top of the valence band to the bottom of the

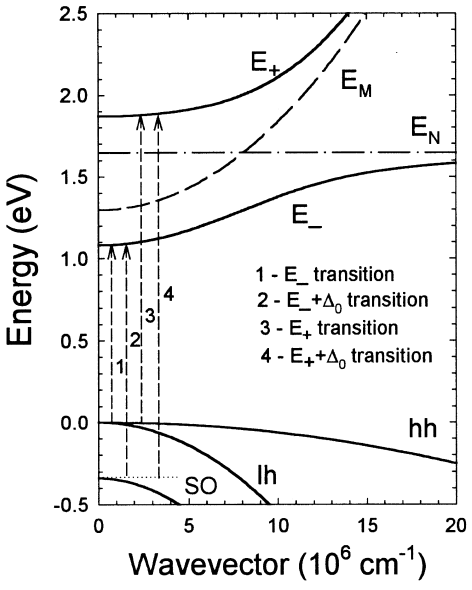

Fig. 1. Dispersion curves for the lower and upper conduction subbands in GaNAs. E_M and E_N represent the unperturbed conduction band of GaAs and the nitrogen level, respectively. The arrows show the possible interband transitions

conduction band and the transition between the spin–orbit split-off band and the conduction-band minimum.

It is evident from Eq. (2) that the initial rate of the N-induced reduction of the band gap depends on the coupling parameter C_{NM} and on the energy difference $E_N - E_M$. Therefore the accurate location of the nitrogen energy level with respect to the conduction band edge is essential to evaluate the effect of N on the band gap reduction in a given material. The existing experimental results on the location of E_N in different group III–V materials indicate that, similar to many other highly localized centers, the energy of the nitrogen level is constant relative to the common energy reference or vacuum level [1, 26]. Therefore using the known conduction band offsets one can determine the energy difference $E_N - E_M$ in III–V compounds and their alloys. For example, based on the well known variation of the band offsets in $Ga_yIn_{1-y}As$ alloys one obtains the following expression for the composition dependent energy of the nitrogen level, $E_N(y) = 1.65 - 0.4y\ (1 - y)$ (eV).

Results and Discussion The predicted splitting of the conduction band into two nonparabolic subbands has been unambiguously observed using photoreflectance (PR) and electro-reflectance (ER) measurements [24, 25]. Figure 2 shows a few representative PR spectra taken from GaN_xAs_{1-x} samples. In the samples with $x > 0$, the E_- and E_+ transitions can be clearly observed. The E_- transition corresponds to the fundamental band gap of GaNAs, and the E_+ transition is related to the new and unique conduction-band edge of GaNAs described by the band anticrossing model in the previous section. E_- shifts down and E_+ shifts up with increasing N content. It is also worth noticing that, as shown in Fig. 2, the spin–orbit splitting energy Δ_0 is equal to $\approx$0.34 eV for all the measured samples and does not depend on N content. The results demonstrate that incorporation of N into GaInAs affects mostly the conduction band and has a negligible effect on the electronic structure of the valence band. The appearance of the new absorption edge E_+ in GaInNAs alloys has also been confirmed through direct absorption measurements on a freestanding GaInNAs film [28].

The observation of E_+ and E_- absorption edges indicate that the BAC model correctly describes the electronic structure of GaInAs alloys. However, the experiments that have provided an unequivocal support for the model were measurements of the

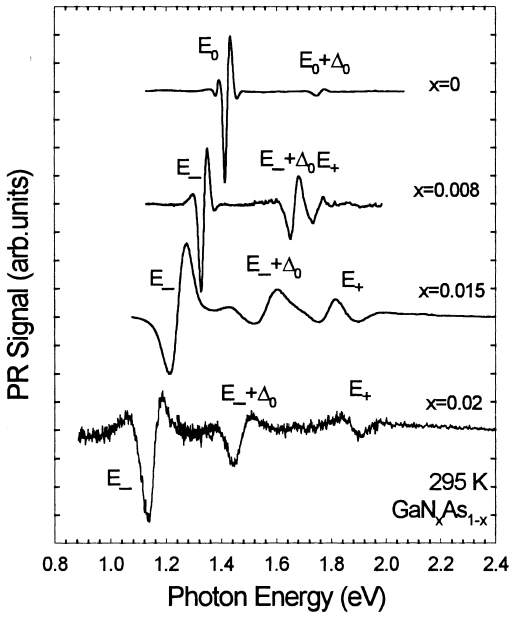

Fig. 2. Photoreflectance (PR) spectra taken from GaN_xAs_{1-x} samples with different N concentrations

pressure dependence of the optical transitions in GaInNAs alloys [24]. Figure 3 shows the measured energies of E_+ and E_- transitions as functions of hydrostatic pressure in a $GaN_{0.015}As_{0.985}$ sample and a $Ga_{0.95}In_{0.05}N_{0.012}As_{0.988}$ sample. It is evident from the data that the E_- and E_+ edges show a classical anticrossing behavior. The experimental results are well explained by the calculations based on the BAC model. We use the well known pressure dependence of the fundamental band gap of the host semiconductor matrices, $dE_M/dP = 10.8$ meV/kbar. Also, based on studies of N doped GaAs we have assumed a small pressure coefficient $dE_N/dP = 1.5$ meV/kbar for the nitrogen levels [2]. The observed pressure dependencies of the absorption edges point at the changing character of the E_- and E_+ transitions. The E_- subband edge which has mostly extended E_M-like character at ambient pressure transforms to a localized E_N-like level at high hydrostatic pressure. On the other hand, E_+ changes its character from localized E_N-like to extended E_M-like at high hydrostatic pressure.

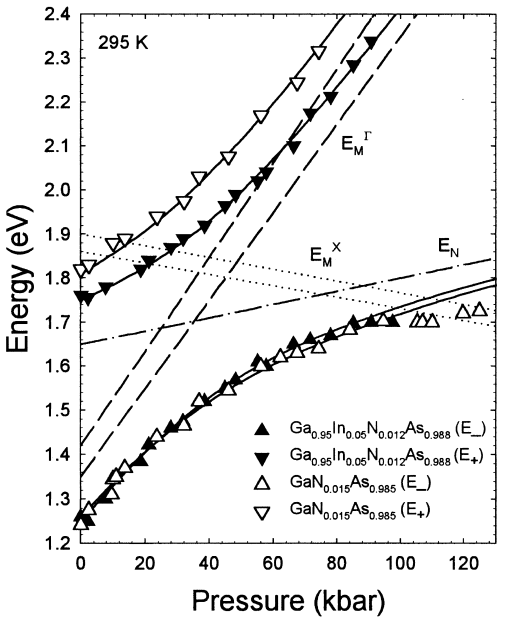

Fig. 3. Effects of pressure on the optical transitions associated with the E_- and E_+ transitions in $GaN_{0.015}As_{0.985}$ and $Ga_{0.95}In_{0.05}N_{0.012}As_{0.988}$

The most extensively studied characteristic of III–N–V alloys has been the dependence of the fundamental band gap on the N content. It was recognized very early that the very rapid reduction of the band gap observed at small N contents cannot be described in terms of standard models with a

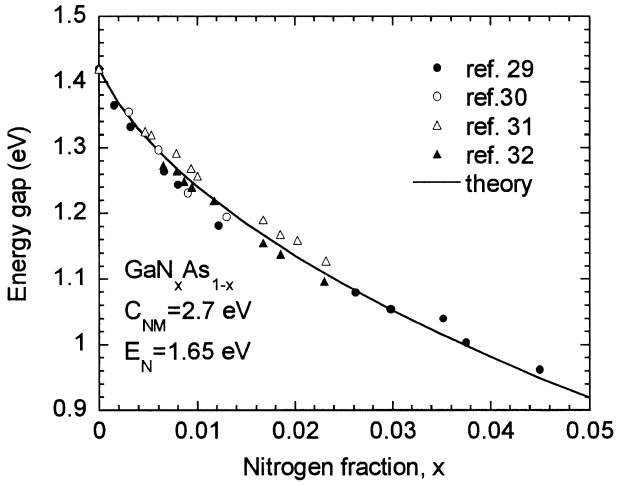

Fig. 4. Experimentally observed dependence of the energy gap on the N fraction in GaN_xAs_{1-x}. The solid line represents the energy gap calculated using the BAC model

composition independent bowing parameter. The failure of this approach is understandable in view of our present results. The energy gap is defined as $E_g = E_-(k = 0)$, where $E_-(k)$ is given by Eq. (2). The calculated band gap as a function of N content in GaN_xAs_{1-x} alloys is shown in Fig. 4. The calculations are in very good agreement with the experimental band gaps reported by different groups [29–32] assuming $C_{NM} = 2.7$ eV. We believe that this comparison with the experiment provides an accurate determination of C_{NM}, which is the only adjustable parameter in the calculations.

The interaction between the localized N states and the extended conduction-band states has a dramatic effect on the dispersion relation $E_\pm(k)$ of the two conduction subbands. As the effect of the interaction is most pronounced for the states located close to E_N, the dispersion relations for the conduction subbands are strongly affected by applying pressure that shifts E_N with respect to the conduction band of the matrix. Figure 5 shows the results of calculations of $E_-(k)$ and $E_+(k)$ for three different values of hydrostatic pressure. It is seen that the pressure has the strongest effect on the lower subband that narrows drastically at high pressures. Narrowing of the band indicates a gradual, pressure-induced transformation in the nature of the lowest subband from an

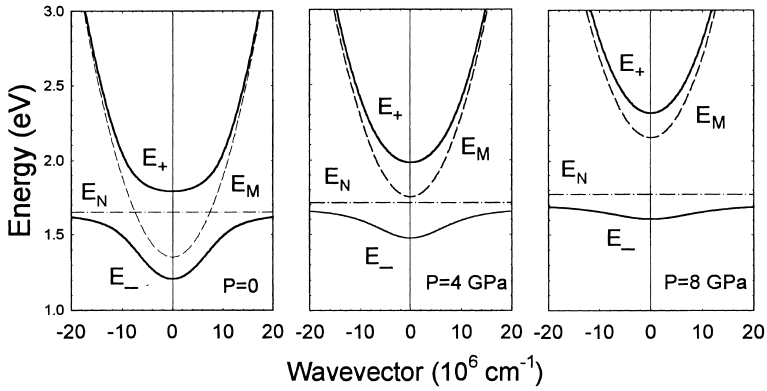

Fig. 5. Calculated dispersion of the E_- and E_+ subbands in GaAsN at three different pressures

extended to a highly localized state. This transformation can also be interpreted as a pressure induced enhancement of the effective mass and the density of states in the lower subband.

The electron effective mass as a function of energy for different pressures can be calculated using the standard definition of the density of states effective mass,

$$m_{\mathrm{eff}} = (h/2\pi)^2\, k(\mathrm{d}E/\mathrm{d}k)^{-1}\,. \tag{6}$$

Using Eqs. (2) and (6), one obtains a simple expression for the effective mass in the lower and upper subbands [27],

$$m_{\mathrm{eff}}(E) = m^*\{1 + [V_{\mathrm{NM}}/(E_{\mathrm{N}} - E)]^2\}\,, \tag{7}$$

where m^* is the effective mass of the semiconductor matrix and E is the energy in the lower or upper subband measured from the valence band edge. It is seen from Eq. (7) that the effective mass diverges for the electron energy approaching E_{N}. This is a result of the increasing contribution of the localized N states to the electron states in the lower and upper subband.

The calculated effective masses for the case of $Ga_{0.92}In_{0.08}N_{0.02}As_{0.98}$ are shown in Fig. 6. There is a very large enhancement of the effective mass as a function of both electron energy and external pressure in the lower subband. An enhancement by almost two orders of magnitude is expected at large hydrostatic pressures. Since the effective mass of the corresponding $Ga_{0.92}In_{0.08}As$ matrix equals $0.06m_0$, the predicted mass can be larger than the free electron mass, m_0 in this case. A large enhancement of the electron effective mass has been recently observed by plasma reflection [33] and magneto-photoluminescence measurements [22]. An electron effective mass as high as $0.4m_0$ has been found in a $Ga_{0.92}In_{0.08}N_{0.033}As_{0.967}$ sample with 6×10^{19} cm^{-3} electrons [33].

It has been predicted that the N-induced downward shift of the conduction band edge and the enhancement of the effective mass in III–N–V alloys should lead to an increase in the maximum electron concentrations that can be achieved by doping [27]. Recent experiments with Se doped GaInNAs alloys have fully confirmed these predictions. For example, an electron concentration of 7×10^{19} cm^{-3} was achieved in a sample

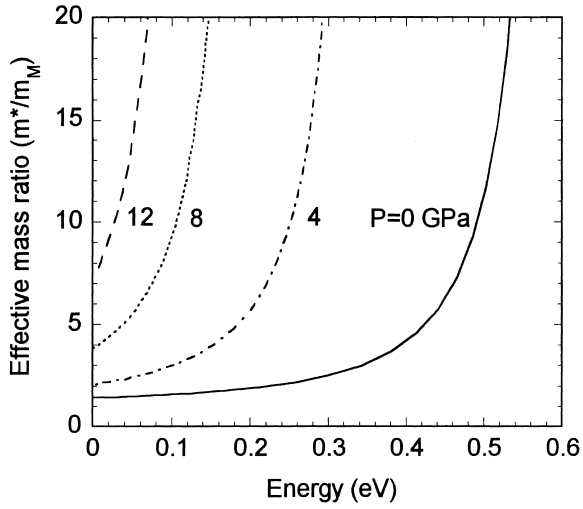

Fig. 6. Dependence of the electron effective mass of the lower subband in $Ga_{0.92}In_{0.08}N_{0.02}As_{0.98}$ on the energy at different values of hydrostatic pressure. The electron effective mass of the GaInAs matrix is $m_{\mathrm{M}} = 0.06\ m_0$

with 3% nitrogen [34]. This value is more than an order of magnitude higher than the electron concentration in Se doped GaAs grown under the same conditions [34].

It has been shown thus far that the band gap reduction in III–N–V alloys can be well modeled by the anticrossing interaction between a narrow band formed by the localized N states and the extended conduction-band states. This approach works very well for the host semiconductor matrix with its conduction band minimum located at the Γ point of the Brillouin zone. However, it has been shown that large N-induced band gap reduction is also found in III–N–V alloys in which the semiconductor matrices have an indirect gap. The most extensively studied alloys of this type have been GaNP; in this system, the nitrogen level is located slightly below the lowest conduction band edge at the X point [5, 8].

Figure 7 shows a PR spectrum of a $GaN_{0.023}P_{0.977}$ sample taken over a wide photon energy range (1.45–3.35 eV). A PR spectrum of GaP is also shown in the figure for comparison. Note that, for the indirect optical transitions such as the Γ_v–X_c transition in GaP as marked by the arrow in the figure, no PR signal is detectable. However, in contrast, two PR spectral features are clearly observed in the $GaN_{0.023}P_{0.977}$ sample. The strong PR feature at 1.96 eV is below the indirect band gap (E_{gX}) of GaP. The weak feature at the energy of 2.96 eV is above the direct bandg ap (E_Γ) of GaP. Similar PR spectra can been observed in all the GaNP samples studied to date. The strong PR signals appear at an energy below the indirect band gap of GaP, indicating a change in the nature of the optical transitions in GaNP and suggesting that the band gap has transformed from indirect in GaP to direct in GaNP. This N-induced transformation from indirect to direct gap can be understood in terms of the band anticrossing model discussed above [35]. It predicts the formation of two subbands $E_-(k)$ and $E_+(k)$ as a result of the interaction of the localized N states and the extended conduction-band states of the GaP matrix. The band gap energy is given by the energy of the lower subband edge, $E_-(0)$, relative to the top of the valence band. The PR spectra of the $GaN_{0.023}P_{0.977}$ sample shown in Fig. 6 are in good agreement with the prediction. The PR spectral feature on the lower energy side can be attributed to the E_- transition. The feature at higher energy can be assigned to the E_+ transition. These data provide direct evidence that the N-induced modification of the conduction band structure is

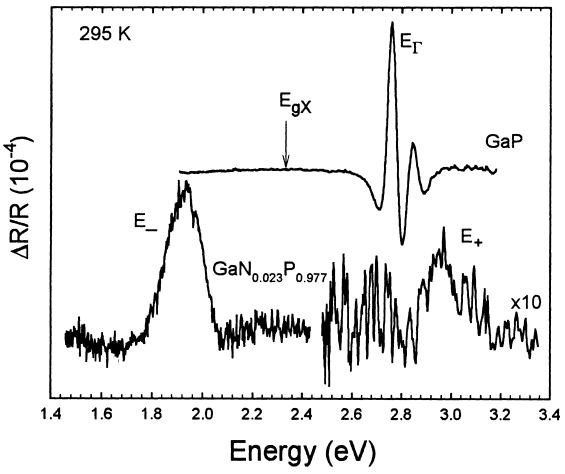

Fig. 7. Comparison between PR spectra of $GaN_{0.023}P_{0.977}$ and GaP. The indirect transition associated with the fundamental band gap (E_{gX}) of GaP cannot be detected by PR measurements

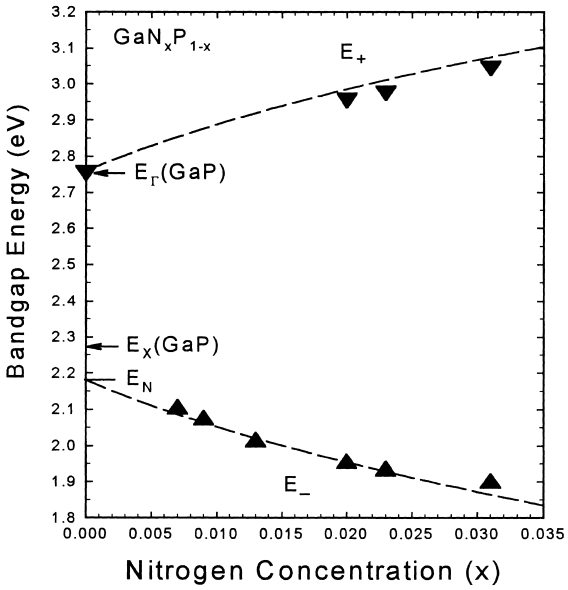

Fig. 8. Energies of the optical transitions in GaNP samples as a function of N concentration. The dashed lines are the calculated variation of the E_- and E_+ edges with N content

dominated by the interaction of the extended states at the conduction band Γ minimum with the N states, even in the case of semiconductor matrices with indirect gaps.

Figure 8 shows the optical transition energies (E_- and E_+) determined by the photomodulation measurements for the GaN_xP_{1-x} samples used in this work. The dashed lines represent the E_- and E_+ transition energies calculated using Eq. (2) with well-known band structure parameters of the GaP matrix: $E_M(\Gamma) = 2.78$ eV, and $E_N = 2.18$ eV. The best fit to the experimental data yields $C_{NM} = 3.05$ eV. This value of the coupling parameter in GaP is about 11% larger than the 2.7 eV determined previously for the GaAs matrix [27].

To further elucidate the role of N in the conduction band structure of GaN_xP_{1-x} alloys, PL transition energies were measured as a function of applied hydrostatic pres-

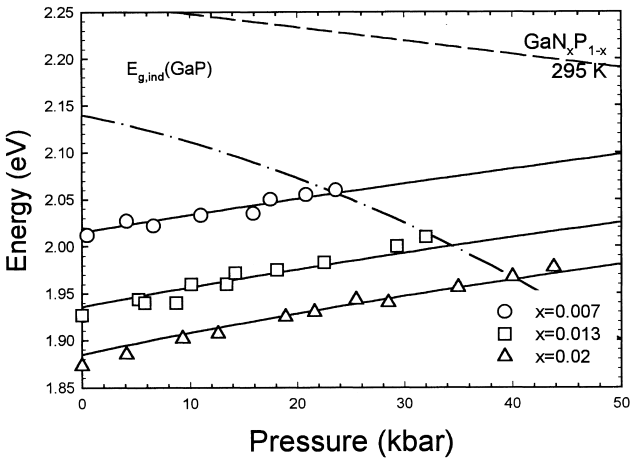

Fig. 9. Pressure dependence of the PL emissions from the GaN_xP_{1-x} samples with $x = 0.007$, 0.013, and 0.02. The solid lines represent the calculated changes of the PL energies. The dashed and dash-dotted lines are two extreme cases of the pressure dependence of the indirect band gap of GaP

sure for samples with three different alloy compositions. The results are shown in Fig. 9. Two extreme cases of the pressure dependence of the indirect band gap (Γ_v–X_c) of GaP are also shown in Fig. 9 [36, 37]. A large reduction of the PL signal was observed at the energies corresponding to the onset of the indirect Γ_v–X_c absorption [37]. The PL emission energies show a small upward shift with increasing pressure. The linear pressure coefficient increases slightly with N content from 2.0 meV/kbar for $x = 0.007$ to 2.53 meV/kbar for $x = 0.02$. The measured pressure coefficients are larger than the pressure coefficient of the highly localized N level, $dE_N/dP = 1.5$ meV/kbar, but much smaller than the pressure coefficient of $dE_{M\Gamma}/dP = 10$ meV/kbar for the $E_{M\Gamma}$ conduction band edge in GaP (see e.g. [38]). This is consistent with the fact that E_- is located much closer to the E_N energy level and its wavefunction has a strong N-like character.

The hydrostatic pressure induced shift of the fundamental bandgap can be calculated by substituting the pressure dependent energy levels $E_N(P)$ and $E_{M\Gamma}(P)$ into Eq. (2). The solid lines in Fig. 9 show the changes of the calculated fundamental band-edge energies. The results are in good agreement with the experimentally observed pressure dependence of the PL emission lines. This provides further support for the band anticrossing model of the conduction band structure of the GaNP alloys. We also recall that the X_c band edge shifts to lower energies with increasing pressure in all known cases of III–V semiconductors. These results again rule out the previous assertions that GaNP has an indirect (Γ_v–X_c) band gap at low N concentrations [5, 6, 17, 21].

Conclusions The effect of N on the electronic band structure in III–N–V alloys has been explained in terms of a band anticrossing interaction between highly localized N states and extended conduction-band states of the semiconductor matrix. The interaction leads to a splitting of the conduction band into two nonparabolic subbands. The downward shift of the lower subband edge relative to the valence band is responsible for the reduction of the fundamental band gap. The N-induced modification of the band structure has profound effects on the optical and electrical properties of the III–N–V alloys.

Acknowledgements This work at LBNL is part of the project on "Photovoltaic Materials Focus Area" in the DOE Center of Excellence for the Synthesis and Processing of Advanced Materials, Office of Science, Office of Basic Energy Sciences, Division of Materials Sciences under U.S. Department of Energy Contract No. DE-AC03-76SF00098. The work at UCSD is partially supported by a UC MICRO program with Rockwell International and the DARPA Heterogeneous Optoelectronics Technology Center.

References

[1] H.P. HJALMARSON, P. VOGL, D.J. WOLFORD, and J.D. DOW, Phys. Rev. Lett. **44**, 810 (1980).
[2] D.J. WOLFORD, J.A. BRADLEY, K. FRY, and J. THOMPSON, in: Physics of Semicondutors, Eds. J.D. CHADI and W.A. HARRISON, Springer, New York 1984 (p. 627).
[3] X. LIU, M.-E. PISTOL, L SAMUELSON, S. SCHWETLICK, and W. SEIFERT, Appl. Phys. Lett. **56**, 1451 (1990).
[4] M. WEYERS, M. SATO, and H. ANDO, Jpn. J. Appl. Phys. **31**, L853 (1992).
[5] J.N. BAILLARGEON, K.Y. CHENG, G. E. HOFLER, P.J. PEARAH, and K.C. HSIEH, Appl. Phys. Lett. **60**, 2540 (1992).
[6] X. LIU, S.G. BISHOP, J.N. BAILLARGEON, and K.Y. CHENG, Appl. Phys. Lett. **63**, 208 (1993).

[7] W.G. Bi and C.W. Tu, J. Appl. Phys. **80**, 1934 (1996).
[8] W.G. Bi and C.W. Tu, Appl. Phys. Lett. **69**, 3710 (1996).
[9] M. Kondow, T. Kitatani, S. Nakatsuka, M.C. Larson, K. Nakahara, Y. Yazawa, M. Okai, and K Uomi, IEEE J. Sel. Top. Quantum Electron. **3**, 719 (1997).
[10] M. Kondow, T. Kitatani, M.C. Larson, K. Nakahara, K. Uomi, and H. Inoue, J. Cryst. Growth **188**, 255 (1998).
[11] W.G. Bi and C.W. Tu, Appl. Phys. Lett. **72**, 1161(1998).
[12] H.P. Xin and C.W. Tu, Appl. Phys. Lett. **72**, 2442 (1998).
[13] G. Pozina, I. Ivanov, B. Monemar, J.V. Thordson, and T.G. Andersson, J. Appl. Phys. **84**, 3830 (1998).
[14] D.J. Friedman, J.F. Geisz, S.R. Kurtz, D. Myers, and J.M Olson, J. Cryst. Growth **195**, 409 (1998).
[15] S.R. Kurtz, A.A. Allerman, E.D. Jones, J.M. Gee, J.J. Banas, and B.E. Hammons, Appl. Phys. Lett. **74**, 729 (1999).
[16] J.A. Van Vechten, Phys. Rev. **187**, 1007 (1969).
[17] J.A. Van Vechten and T.K. Bergstresser, Phys. Rev. B **1**, 3351 (1970).
[18] A. Rubio and M.L. Cohen, Phys. Rev. B **51**, 4343 (1995).
[19] J. Neugebauer and C.G. Van de Walle, Phys. Rev. B **51**, 10568 (1995).
[20] S.-H. Wei and A. Zunger, Phys. Rev. Lett. **76**, 664 (1996).
[21] L. Bellaiche, S.-H. Wie, and A. Zunger, Phys. Rev. B **54**, 17568 (1996); **56**, 10233 (1997).
[22] E.D. Jones, N.A. Modine, A.A. Allerman, S.R. Kurtz, A.F. Wright, S.T. Tozer, and X. Wei, SPIE Proc. **3621**, 52 (1999); Phys. Rev. B **60**, 4430 (1999).
[23] T. Mattila, S.H. Wei, and A. Zunger, Phys. Rev. B **60**, R11245 (1999).
[24] W. Shan, W. Walukiewicz, J.W. Ager III, E.E. Haller, J.F. Geisz, D.J. Friedman, J.M. Olson, and S.R. Kurtz, Phys. Rev. Lett. **82**, 1221 (1999); J. Appl. Phys. **86**, 2349 (1999).
[25] J.D. Perkins, A. Mascarenhas, Y. Zhang, J.F. Geisz, D.J. Friedman, J.M. Olson, and S.R. Kurtz, Phys. Rev. Lett. **82**, 3312 (1999).
[26] Y. Makita, H. Ijuin, and S. Gonda, Appl. Phys. Lett. **28**, 287 (1976).
[27] W. Walukiewicz, W. Shan, J.W. Ager III, D.R. Chamberlin, E.E. Haller, J.F. Geisz, D.J. Friedman, J.M. Olson, and S.R. Kurtz, Electrochem. Soc. Proc. Vol. (USA) **99-11**, 190 (1999).
[28] P. Perlin, P. Wisniewski, C. Skierbiszewski, T. Suski, E. Kaminska, S.G. Subramanya, E.R Weber, D. E Mars, and W. Walukiewicz, Appl. Phys. Lett. **76**, 1279 (2000).
[29] K. Uesugi, N. Marooka, and I. Suemune, Appl. Phys. Lett. **74**, 1254 (1999).
[30] B.M. Keyes, J.F. Geisz, P.C. Dippo, R. Reedy, C. Kramer, D.J. Friedman, S.R. Kurtz, and J.M. Olson, NCPV Photovoltaics Program Review, AIP Conf. Proc. **462**, 511 (1999).
[31] L. Malikova, F.H. Pollak, and R. Bhat, J. Electron. Mater. **27**, 484 (1998).
[32] R. Bhat, C. Caneau, L. Salamanca-Riba, W. Bi, and C. Tu, J. Cryst. Growth **195**, 427 (1998).
[33] C. Skierbiszewski, P. Perlin, P. Wisniewski, W. Knap, T. Suski, W. Walukiewicz, W. Shan, K.M. Yu, J.W. Ager, E.E. Haller, J.F. Geisz, and J.M. Olson, Appl. Phys. Lett. **76**, 2409 (2000).
[34] K.M. Yu, W. Walukiewicz, W. Shan, J.W. Ager III, J. Wu, E.E. Haller, J.F. Geisz, D.J. Friedman, and J.M. Olson, Phys. Rev. B **61**, R13 337 (2000).
[35] W. Shan, W. Walukiewicz, K.M. Yu, J. Wu, J.W. Ager, E.E. Haller, H.P. Xin, and C.W. Tu, Appl. Phys. Lett. **76**, 3251 (2000).
[36] S. Ves, K. Strossner, C.K. Kim, and M. Cardona, Solid State Commun. **55**, 327 (1985).
[37] A.R. Goni, K. Syassen, K. Strossner, and M. Cardona, Phys. Rev. B **39**, 3178 (1989).
[38] G. Martinez, in: Optical Properties of Solids, Ed. M. Balkanski, North-Holland, Amsterdam 1980 (Chap. 4C).